

SERI/TP-211-1391
UC Category: 60c

A Parametric Study of Tornado-Type Wind Energy Systems

S. S. Ayad

October 1981

**Presented at Wind Workshop V;
Washington, D.C.; 5-8 October 1981;
Sheraton Hotel**

**Prepared under Task No. 1067.15
WPA No. 172-81**

Solar Energy Research Institute

A Division of Midwest Research Institute

1617 Cole Boulevard
Golden, Colorado 80401

Prepared for the
U.S. Department of Energy
Contract No. EG-77-C-01-4042

Printed in the United States of America
Available from:
National Technical Information Service
U.S. Department of Commerce
5285 Port Royal Road
Springfield, VA 22161
Price:

Microfiche \$3.00
Printed Copy \$ 4.00

NOTICE

This report was prepared as an account of work sponsored by the United States Government. Neither the United States nor the United States Department of Energy, nor any of their employees, nor any of their contractors, subcontractors, or their employees, makes any warranty, express or implied, or assumes any legal liability or responsibility for the accuracy, completeness or usefulness of any information, apparatus, product or process disclosed, or represents that its use would not infringe privately owned rights.

A PARAMETRIC STUDY OF TORNADO-TYPE WIND ENERGY SYSTEMS

S. S. Ayad

Mechanical Engineering Department
Faculty of Engineering at Shobra, Cairo, Egypt

ABSTRACT

The tornado-type wind energy system uses the pressure drop created by an intense vortex. The vortex is generated in a tower mounted at the turbine exit. The tower serves as a low pressure exhaust for the turbine. In a previous work, the author provided a numerical solution, using the two-equation ($k-\epsilon$) turbulence model, of the tower flow with a uniform wind flow. Results compared favorably with measured values of pressure and showed a turbine diameter of ~ 0.4 times that of the tower to be optimum. In the present work, the author provides results to show the effects of embedding the tower in an atmospheric boundary layer, varying the tower height to diameter ratio, and varying tower diameter using the same system geometry and approach flow conditions. The results indicate a reduction of $\sim 28\%$ in power output caused by atmospheric boundary layer effects using a power law profile, a minimum height/diameter ratio of ~ 1.0 to avoid asymmetric vortex decay, and decreasing improvements in system performance with increasing system size. For the latter, the results show a 23% increase in the power coefficient by increasing the tower diameter from 0.5 m to 1.0 m, but only a 1% increase by increasing the tower diameter from 4 m to 8 m.

INTRODUCTION

Several investigators have considered using the vortex flow to create a region of low pressure at the exhaust of the turbine [1-6]. The tornado-type wind energy system is one of several concepts being investigated under the wind energy program of the U.S. Department of Energy. The system uses the low pressure created at the core of an intense vortex to increase the energy flux through the turbine. The vortex is generated inside a tower mounted at the turbine exit.

Yen [5] tested a small model of the tornado-type wind energy system in a small, uniform flow wind tunnel. The model has a tower of 0.127-m diameter and 0.35-m height and was tested in a wind tunnel with a

cross section of $0.6 \text{ m} \times 0.9 \text{ m}$. He examined the flow in a closed-bottom tower and a tower with simulated turbine flows. He measured the radial distributions of pressure and estimated the power coefficients. The author [7] developed a numerical model for the flow within the small system tower investigated by Yen [5], (Fig. 1) using the two-equation turbulence model to predict the mean values of the three components of velocity and the pressure for the tower flow. Two transport equations for the kinetic energy of turbulence per unit mass k and its rate of dissipation ϵ were solved simultaneously with the basic equations for momentum and continuity. Figures 2 and 3 show the comparison of the resulted pressure distribution for the closed-bottom tower and the power coefficient for the simulated turbine case with those measured by Yen [5]. The comparisons show that the model is adequate for predicting mean flow values and system performance. Also analyzed were the effect of the axial turbine flow into the tower on the vortex strength. The model showed that the calculations based on the closed-bottom tower over estimated the power coefficient of the system. The results also showed that a turbine of 0.38 times that of the tower is optimum for the system analyzed. Axial flows from larger turbines destroy the vortex low pressure at low levels in the tower.

Present work concentrates on the effects of the atmospheric boundary layer, the tower height-to-diameter ratio, and the system size on the performance of a tornado-type wind energy system. Numerical solutions of the basic equations for the turbulent flow in the tower is carried out for each flow condition using the two-equation turbulence model for the closure.

THE BASIC EQUATIONS

The author used a cylindrical flow domain of radius R_0 and height H_d , which included a vortex decay region from the tower height

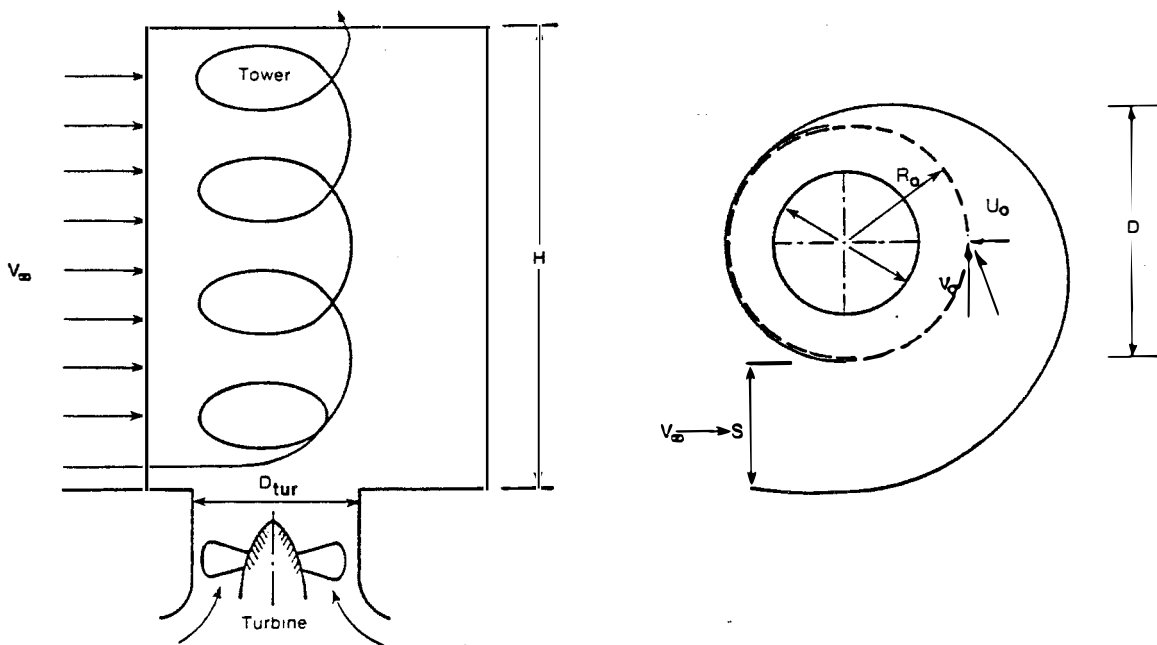


Figure 1. Sketch of a Model for the Tornado-Type Wind Energy System [7]

H up to H_d . A simulated turbine flow jet of radius R_{tur} was assumed to be located concentrically with the tower at its bottom. Figure 4 shows the computational domain together with the boundary conditions and the mesh definition. The flow was assumed to be incompressible and axisymmetric. The assumption of axisymmetry within the tower was supported by the pressure measurement of Yen [5] at different angular locations. The asymmetric effects on the flow as it exits the tower will be discussed later. The appropriate equations for analysis follow:

Mass Conservation

$$\frac{1}{r} \frac{\partial}{\partial r} (Ur) + \frac{\partial W}{\partial z} = 0 \quad [1]$$

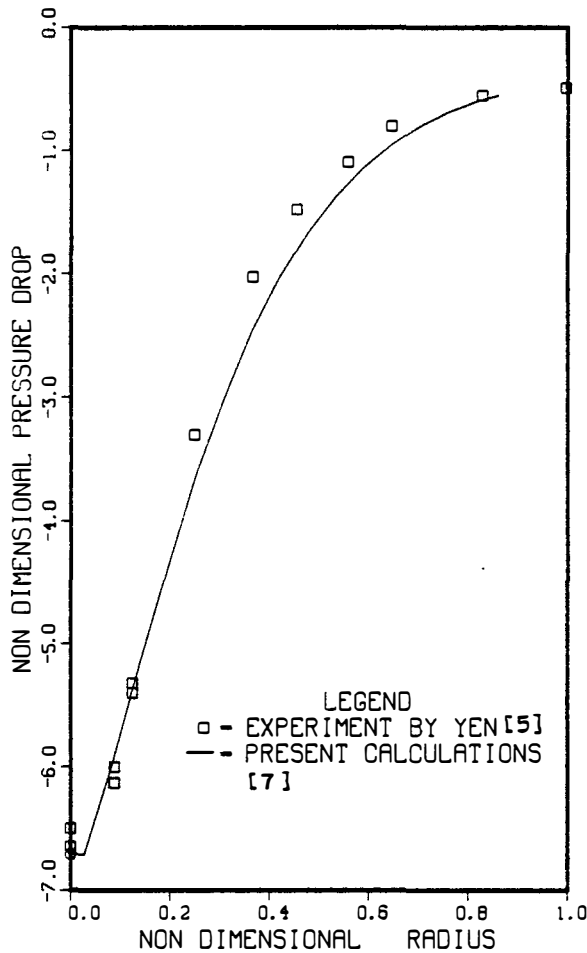


Figure 2.

Radial Distribution of Pressure Drop at the Bottom of the Closed Bottom Tower, Values Normalized by $1/2 (\rho V_0^2)$ [7]

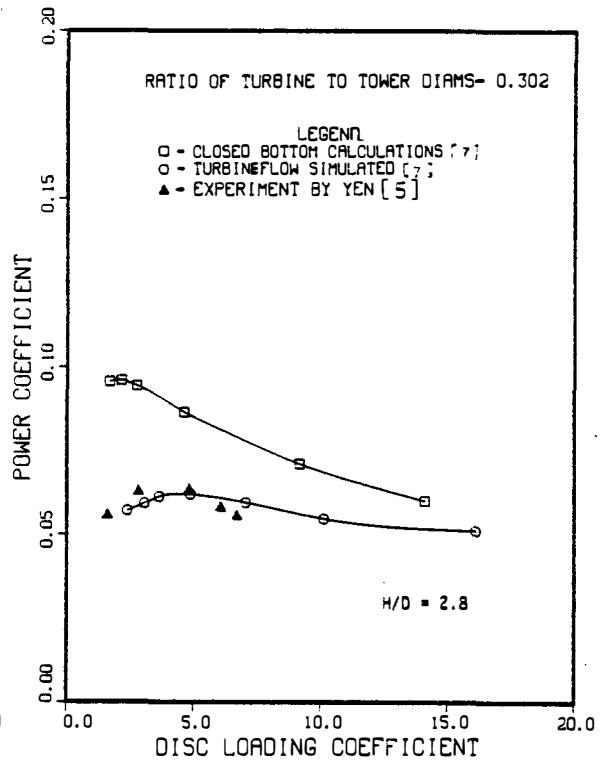


Figure 3.

Comparison Between Power Coefficient Obtained for Closed Bottom Tower, Tower with Simulated Turbine Flow and Experiment by Yen [5]

Radial Momentum

$$\frac{\partial U}{\partial t} + \frac{1}{r} \frac{\partial (U^2 r)}{\partial r} + \frac{\partial (UW)}{\partial z} - \frac{v^2}{r} = -\frac{1}{\rho} \frac{\partial p}{\partial r} + \frac{1}{\rho r} \frac{\partial}{\partial r} \left(2r\mu_{\text{eff}} \frac{\partial U}{\partial r} \right) + \frac{\partial}{\partial z} \left[\mu_{\text{eff}} \left(\frac{\partial U}{\partial z} + \frac{\partial W}{\partial r} \right) \right] - 2 \frac{\mu_{\text{eff}}}{\rho} \left(\frac{U}{r^2} \right) \quad [2]$$

Tangential Momentum

$$\frac{\partial V}{\partial t} + \frac{1}{r} \frac{\partial}{\partial r} (rUV) + \frac{\partial}{\partial z} (WV) + \frac{UV}{r} = \frac{1}{\rho} \frac{\partial}{\partial z} \left(\mu_{\text{eff}} \frac{\partial V}{\partial z} \right) + \frac{1}{\rho r^2} \frac{\partial}{\partial r} \left[r^3 \mu_{\text{eff}} \frac{\partial (V/r)}{\partial r} \right] \quad [3]$$

Axial Momentum

$$\frac{\partial W}{\partial t} + \frac{1}{r} \frac{\partial (Wru)}{\partial r} + \frac{\partial (W^2)}{\partial z} = -\frac{1}{\rho} \frac{\partial p}{\partial z} + \frac{1}{\rho} \frac{\partial}{\partial z} \left(2\mu_{\text{eff}} \frac{\partial W}{\partial z} \right) + \frac{1}{\rho r} \frac{\partial}{\partial r} \left[r\mu_{\text{eff}} \left(\frac{\partial U}{\partial z} + \frac{\partial W}{\partial r} \right) \right] - g \quad [4]$$

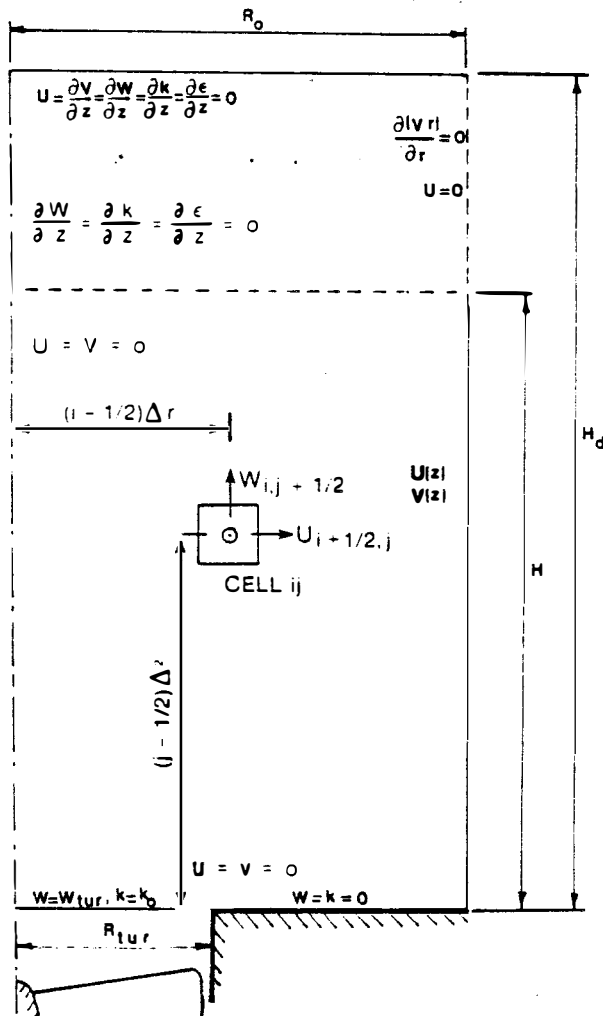


Figure 4.

The Computational Domain for the Tower of the Tornado-Type Wind Energy System with a Decay Region

The gradient model of turbulence is employed with an effective viscosity μ_{eff} :

$$\mu_{\text{eff}} \equiv C_{\mu} \frac{\rho k^2}{\varepsilon} + \mu \quad .$$

The values of the kinetic energy of turbulence k and its rate of dissipation ε are obtained from the solutions of their following respective transport equations.

Transport Equation for Kinetic Energy of Turbulence

$$\begin{aligned} \rho \frac{\partial k}{\partial t} + \frac{1}{r} \frac{\partial}{\partial r} (Ukr) + \frac{\partial}{\partial z} (Wk) \\ = P_s + \frac{\partial}{\partial z} \left[\left(\mu + \frac{\mu_T}{\sigma_k} \right) \frac{\partial k}{\partial z} \right] + \frac{1}{r} \frac{\partial}{\partial r} \left[\left(\mu + \frac{\mu_T}{\sigma_k} \right) \frac{r \partial k}{\partial r} \right] - \rho \varepsilon \quad . \end{aligned} \quad [5]$$

Transport Equation for Turbulence Dissipation

$$\begin{aligned} \rho \left[\frac{\partial \varepsilon}{\partial t} + \frac{1}{r} \frac{\partial}{\partial r} (U\varepsilon r) + \frac{\partial}{\partial z} (W\varepsilon) \right] = \frac{\varepsilon}{k} C_1 P_s \\ + \frac{\partial}{\partial z} \left[\left(\mu + \frac{\mu_T}{\sigma_{\varepsilon}} \right) \frac{\partial \varepsilon}{\partial z} \right] + \frac{1}{r} \frac{\partial}{\partial r} \left[r \left(\mu + \frac{\mu_T}{\sigma_{\varepsilon}} \right) \frac{\partial \varepsilon}{\partial r} \right] - C_2 \rho \frac{\varepsilon^2}{k} \end{aligned} \quad [6]$$

where

$$\begin{aligned} P_s = \mu_T \left\{ 2 \left[\left(\frac{\partial U}{\partial r} \right)^2 + \left(\frac{\partial W}{\partial z} \right)^2 + \left(\frac{U}{r} \right)^2 \right] \right. \\ \left. + \left(\frac{\partial U}{\partial z} + \frac{\partial W}{\partial r} \right)^2 + \left(\frac{\partial V}{\partial z} \right)^2 + r^2 \left[\frac{\partial (V/r)}{\partial r} \right]^2 \right\} \end{aligned}$$

is the production of turbulence energy due to shear. Reoptimized by Launder and Sharma [8], the coefficients C_1 , C_2 , and C_{μ} are given by

$$\begin{aligned} C_1 &= 1.42 \\ C_2 &= 1.92 [1 - 0.3 \exp(-R_t^2)] \\ C_{\mu} &= 0.09 \exp[-3.4/(1 + R_t^2/50)^2] \end{aligned}$$

To solve Eqs. 1-6 numerically, the boundary conditions should be specified on all the boundaries of the flow domain.

Boundary Conditions

At $r = 0$ and for any z ,

$$U = V = \frac{\partial W}{\partial r} = \frac{\partial p}{\partial r} = \frac{\partial k}{\partial r} = \frac{\partial \varepsilon}{\partial r} = 0 \quad .$$

At $r = R_0$ and any z , $k = k_0$ and $\partial \varepsilon / \partial r = \partial W / \partial r = 0$.
At $r = R_0$ and for $0 < z < H$,

$$U = U_0(z) \quad \text{and} \quad V = V_0(z)$$

The profiles of $U_0(z)$ and $V_0(z)$ at the side boundary were specified according to the approaching wind velocity profile. Their relative

values depended on the geometry of the tower inlet. Based on the pressure values in the spiral tower measured by Yen [5] and the discussion in [7], the values of $V_o(z) = 0.76 V_\infty(z)$ were used for all the results reported. The values of $V_o(z)/U_o(z) = 5.25$ and k_o that corresponds to 6% turbulence are used for the results reported.

The region above the tower height H and up to H_d is a vortex decay region where the vortex is allowed to decay symmetrically with no inflow and irrotational vortex condition at the side boundary. H_d is taken to be $1.5 H$. At $r = R_o$ and $H < z < H_d$

$$U = \frac{\partial(rv)}{\partial r} = 0 \quad .$$

At $z = 0$ and for any r , $U = V = 0$. At $z = 0$ and for $0 \leq r < R_{tur}$, $W = W_{tur}$ and $k = k_o$. At $z = 0$ and for $R_{tur} \leq r < R_o$, $W = 0$ and $k = 0$.

To avoid using large numbers of nodal points in the vertical direction near the closed portion of the tower (following Chieng and Launder [9]), the kinetic energy of turbulence was assumed to increase proportional to z^2 from zero at $z = 0$, to a value k_v at a height z_v , such that

$$\frac{z_v(k_v)^{1/2}}{\nu} = 20 \quad .$$

The turbulent tangential shear stress at the top of the viscous sub-layer was calculated and used in the tangential momentum equation and the production term of the turbulence energy transport equation. To estimate the radial turbulent shear stress near the wall, the effect of the imbalance between the radial pressure gradient and the centrifugal force was used:

$$\frac{1}{r} \frac{\partial(\overline{u'w'})}{\partial z} = \frac{\nu^2}{r} - \frac{1}{\rho} \frac{\partial P}{\partial r} \quad . \quad [7]$$

The dissipation rate ϵ at point p , the first nodal point next to the wall, was assumed to be

$$\epsilon_p = C_D k^{(3/2)} / \ell_D \quad ,$$

where

$$\ell_D = z_p(1 - 5R_i) \quad .$$

and R_i is a swirl-Richardson number to include the effect of swirl on the boundary value of ϵ [10].

At $z = H$ for any r , $\partial p / \partial z$ was obtained from Eq. 4 for axial momentum and the radial flow was assumed to vanish and free-slip conditions for v and w were considered,

$$U = \frac{\partial V}{\partial z} = \frac{\partial W}{\partial z} = \frac{\partial k}{\partial z} = \frac{\partial \epsilon}{\partial z} = 0 \quad ,$$

Numerical Solution

An explicit finite difference method centered in space and time with a leap-frog scheme was used on a staggered mesh. The flow domain was

divided into 26 cells radially by 96 cells vertically. The momentum equations were solved in their primitive form and an interactive solution for the pressure was employed such that the velocity divergence vanishes everywhere. Diffusion terms were delayed by one time step to avoid instability, and a forward time step was carried out every hundred steps to avoid computational separation. The iteration continued until a steady-state solution was reached for all the variables.

When the details of pressure distribution and velocity field are obtained; the maximum power P that can be extracted using the low pressure of the vortex was calculated using the axial thrust on the turbine disc:

$$P = 2\pi \int_0^{R_{tur}} W_{tur}(r) [p_{\infty} - p_t(r)] r dr \quad . \quad (8)$$

Total axial thrust T was given by:

$$T = 2\pi \int_0^{R_{tur}} [p_{\infty} - p_t(r)] r dr \quad . \quad (9)$$

The total pressure at the turbine exit $P_t(r)$ at any radius r is assumed to be

$$p_t(r) = p(r) + \frac{1}{2} \rho W_{tur}^2 r \quad .$$

The total pressure at the turbine inlet was assumed to equal the free steam pressure P_{∞} , simulating the case where the turbine is not exposed to the free wind velocity. Equations 8 and 9 were integrated numerically across the turbine radius.

The disc loading coefficient and the power coefficient, based on tower frontal area HD , were defined as

$$C_T \equiv \frac{T}{\frac{1}{2} \rho W_{tur}^2 \pi R_{tur}^2} \quad ,$$

and

$$C_P \equiv \frac{P}{\frac{1}{2} \rho V_{\infty}^3 HD} \quad ,$$

respectively. The power coefficient based on turbine area C_{pt} , used to compare cases with variable tower heights, was defined as

$$C_{pt} \equiv \frac{P}{\frac{1}{2} \rho V_{\infty}^3 \pi R_{tur}^2} \quad .$$

MODEL RESULTS

Calculations of the flow variables and the corresponding potential power outputs of the tornado-type wind energy system were performed to

show the effects of an atmospheric boundary layer, the tower height-to-diameter ratio, and size on system performance. The present section summarizes the results found when varying these parameters.

The Effect of Atmospheric Boundary Layer

The experimental results by Yen [5] and the results of the numerical model present in [7] are for a tower in a wind stream of uniform velocity. From a practical point of view, the tower of the tornado-type wind energy system will be embedded in the atmospheric boundary layer. The height of the boundary layer may vary according to the topography of the area and averages 300-600 m. The exhaust pressure imposed on the turbine by the vortex is expected to be more sensitive to the flow in the lower portion of the tower where large vertical gradients of the wind velocity occur. Figure 5 shows the power coefficients for both cases of tower in a uniform wind of velocity of $V = V_\infty$ and that in a typical boundary layer of a power-law profile with V_∞ at the top of the tower

$$\frac{V(z)}{V_\infty} = \left(\frac{z}{H}\right)^{1/7}$$

The results are plotted for a tower diameter of 0.5 m and $V_\infty = 5.7$ m/sec. Figure 5 shows the reduced values of power coefficient that amounts up to 28% because of the boundary layer. This reduction in power is a result of the reduced circulation in the lower portion of the tower. At $z = 0.45H$ for the boundary layer profile, caused by a power reduction of 28%, the velocity (thus the circulation) and the wind power flux are 89.5% and 72% of their uniform stream values, respectively. Note, that if a reference

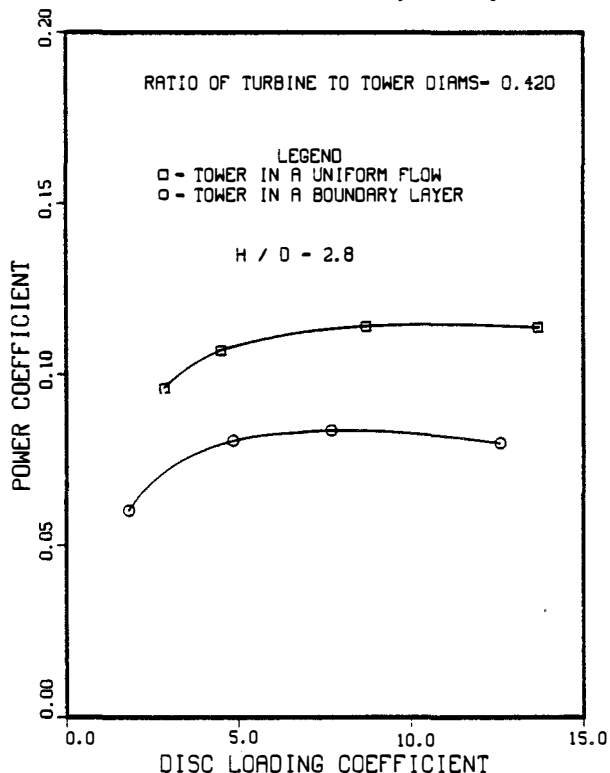


Figure 5.

Effect of Atmospheric Boundary Layer on the Power Coefficient

velocity at $z/H = 0.45$ is used for computing C_p , the values of C_p with and without wind shear will be identical. For small towers with diameters of a few meters, the tower will be embedded in the atmospheric surface layer where the shear stress is almost constant and the logarithmic velocity profile will hold for the thermally-neutral atmospheric condition. Thus the performance of the system will depend on the aerodynamic roughness of the surrounding area z_0 .

Effects of the Tower Height-to-Diameter Ratio

To find the optimum tower height for given tower and turbine diameters, the tower flow and the possible power extraction were calculated using fixed tower and turbine diameters. The turbine diameter used, based on the results in [7], was 0.4 times that of the tower. The tower was assumed to be embedded in an atmospheric boundary layer of a power-law profile ($n = 1/7$) with a boundary layer thickness of 3.8 times the tower diameter. As given in Fig. 4, the vortex was permitted to decay symmetrically for heights of $z > H$ where the radial velocity at the side boundary vanishes. Note that such symmetric decay will maintain the vortex at heights well above the tower ($z = H$), and the asymmetric effects, which were not considered in the present model, may result in a faster decay.

Figure 6 shows the variation of the power coefficient based on the turbine area, C_{pt} , with the ratio of H/D . Values are calculated at a disc loading coefficient $C_T = 4.5$. To keep C_T unchanged W_{tur}/V_∞ had to be varied between 0.68 to 0.52 with the smaller values for towers of smaller H/D . Figure 6 shows that a sharp decrease of the power output takes place for $H/D \leq 0.5$ with about 50% power decrease for $H/D = 0.25$.

The tangential velocity profiles for the limiting case of $H/D = 0.54$ are plotted in Fig. 7. The figure shows that for the symmetric model, the vortex will not completely decay until $z/D > 0.9$. To avoid the asymmetric decay, the tower height may have to be increased beyond the limiting value of 0.5 of tower diameter and a tower of $H/D = 1$ is recommended.

Figure 8 shows the variation of the power coefficient based on the tower frontal area HD with the ratio of tower height to its diameter. Although the figure shows an increase of C_p with the decrease of H/D down until $H/D \approx 0.25$, the total power generated by the system decreases with the decrease of H/D below $H/D = 0.5$ and is expected to decrease with the decrease of H/D below ~ 0.9 for the asymmetric case.

Effects of System Size

Numerical predictions were also made for systems with tower diameters that vary between 0.5-8 m, (1.64-26.24 ft). The same system geometry, using a turbine-to-tower diameter ratio of 0.4 and a tower height-to-diameter ratio of 1, as well as the same approach wind conditions, using a power-law profile with V_∞ at $z = 3.8 H$ and a $1/7$ exponent,

were used in the calculations. The results, shown in Fig. 9, indicate that improving performance by increasing system size is possible for tower diameters $< \sim 8$ m. However, the rate of improvement decreases with system size in this range. For example, an increase in tower diameter of 0.5 m to 1.0 m improves system performance by 23%. However, diameter increases from 2 m to 4 m and 4 m to 8 m only cause performance improvements of 5% and 1%, respectively. Thus, performance appears to be independent of system size for tower diameters > 8 m. Figure 10 shows the extractable power per unit area of the tower as a function of wind speed for the two cases of 0.5-m and 4-m diameter towers. Also shown is the extractable power per unit tower area based on the Betz limit.

CONCLUSIONS

The two-equation ($k-\epsilon$) turbulence model has been used to predict the flow through tornado-type wind energy systems. The model was previously verified by comparing with experimental results. The present study shows the following conclusions:

- the atmospheric boundary layer has a severe effect on the system performance;
- the vortex has to be maintained in the tower up to a height of one tower diameter to prevent power losses due to vortex decay as it exits the tower;

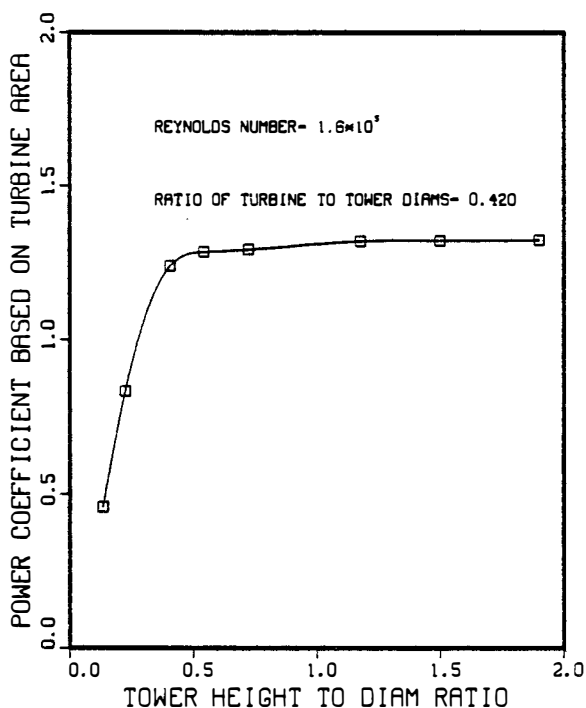


Figure 6.

Variations of the Power to be Extracted with the Tower Height-to-Diameter Ratio

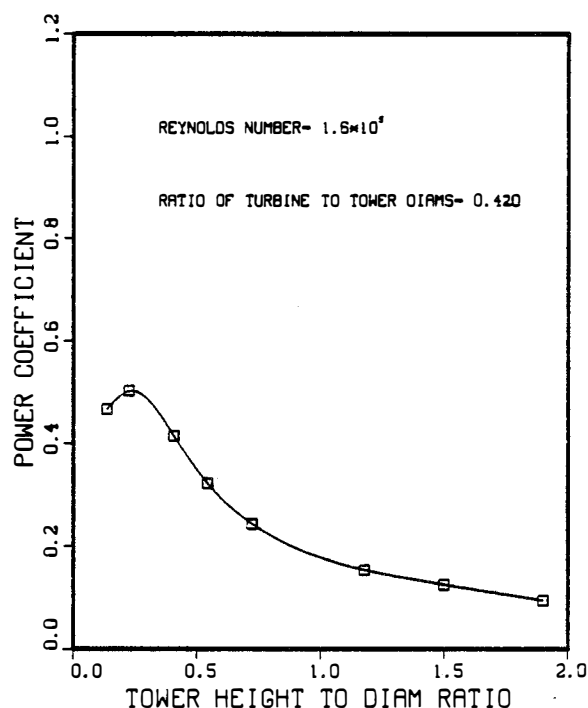


Figure 7.

Variation of Power Coefficient with Tower Height-to-Diameter Ratio

- the performance of small systems improves as the size increases. However, for 8 m diameter towers or larger, performance appears to be independent of system size.

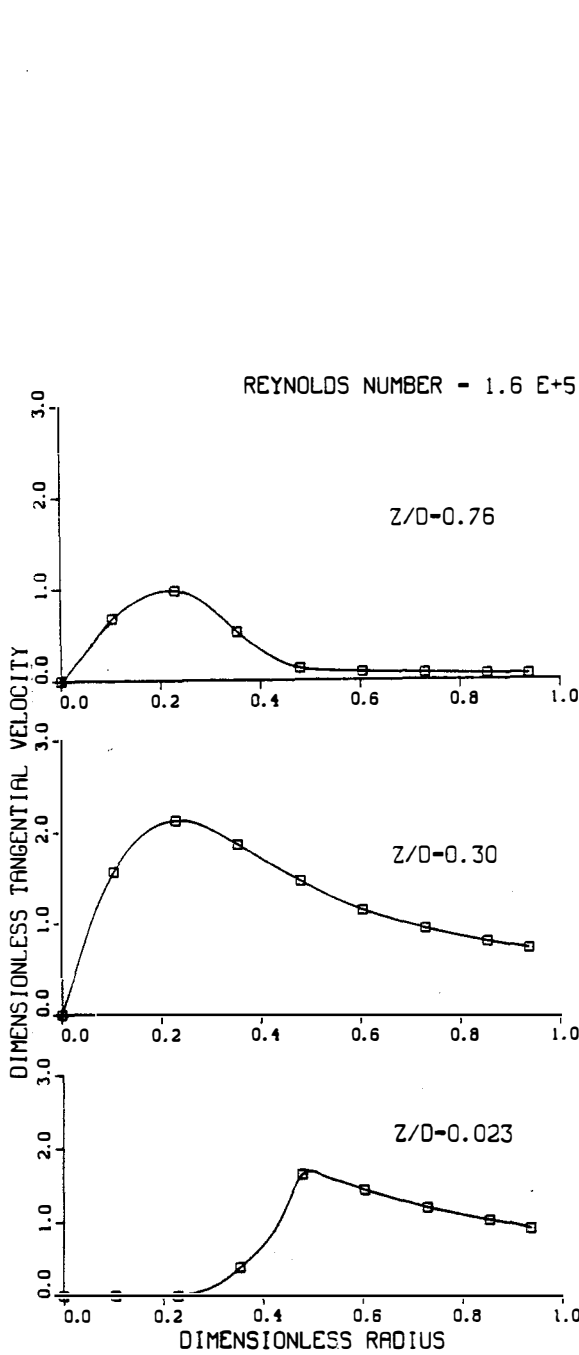


Figure 8.

Radial Distributions of Tangential Velocity at Different Levels in the Tower of a Tornado-Type Wind Energy System

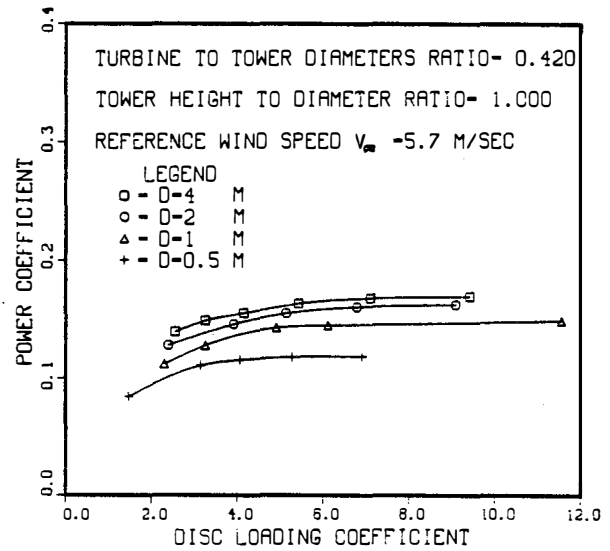


Figure 9.

Effect of Systems Size on the Performance of Tornado-Type Wind Energy Systems

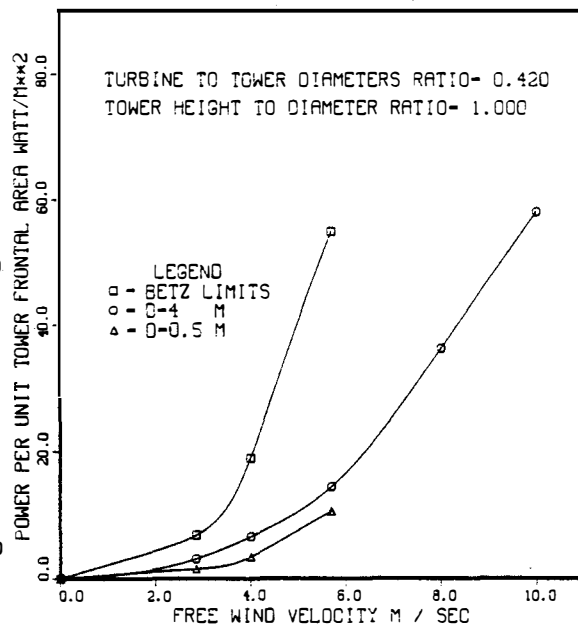


Figure 10.

Variation of the Power to be Extracted by the Tornado-Type Wind Energy System with Free Wind Velocity, V_{ref} .

ACKNOWLEDGMENTS

I would like to express my gratitude to Irwin Vas, Peter South, and Eric Jacobs of the Solar Energy Research Institute (SERI), all of whom introduced me to tornado-type wind energy systems. Thanks are also due to Professor J. E. Cermak of Colorado State University, for his continuing advice and support. The work was supported by the Wind Energy Innovative Systems Program at SERI for the U.S. Department of Energy under contract No. EG 77-C-01-4042.

REFERENCES

1. Yen, J. T. 1976 (Sept.). "Tornado-Type Wind Energy System Basic Considerations." Paper E4, International Symposium on Wind Energy System. BHRA, Cambridge, England, pp. 47-64.
2. Loth, J. L. 1978. "Wind Power Limitations Associated with Vortices." Journal of Energy. Vol. 2 (July-August): p. 216-222.
3. So, R. M. C. 1978. "On the Vortex Wind Power." Journal of Fluids Engineering. Vol. 100 (March): pp. 79-82.
4. Hsu, C. T.; Mellor, G. L.; Yen, J. T. 1978. "Some Flow Analyses for Tornado-Type Wind Turbines." Fluids Engineering in Advanced Energy System. Presented at the ASME 1978 Winter meeting. 78-S9988. pp. 59-71.
5. Yen, J. T. 1977. "Summary of Recent Progress on Tornado-type Wind Energy System." Proceedings of the Third Biennial Conference and Workshop on Wind Energy Conversion Systems. Vol. 2, Washington, D.C. Sept. 19-21, pp. 808-817.
6. Chen, J. M. 1978. "Vortex Affected by the Conical Shape of Generator in Tornado-Type Wind Energy System." Journal of Industrial Aerodynamics. Vol. 3: pp. 307-313.
7. Ayad, S. S. 1981. "A Numerical Model for the Flow Within the Tower of Tornado-type Wind Energy System." To be published in the Journal of Solar Energy Engineering.
8. Launder, B. E. and Sharma, B. I. 1974. "Application of Energy-Dissipation of Turbulence to the Calculation of Flow Near a Spinning Disc." Letters in Heat and Mass Transfer. Vol. 1: pp. 131-138.
9. Chieng, C. C. and Launder, B. E. 1981. "On the Calculation of Turbulent Heat Transport Downstream from an Abrupt Pipe Expansion." Presented at the Winter Annual Meeting of the American Society of Mechanical Engineers, Chicago, IL, Nov. 16-21, pp. 9-19.
10. Ayad, S. S. 1980. "A Turbulence Model for Tornado-Like Swirling Flow." Ph. D. Dissertation, Fluid Mechanics and Wind Engineering Program, Colorado State University, Fort Collins, CO.

NOMENCLATURE

a	the vortex core radius	R_t	turbulence Reynolds number, $R_t \equiv k^2/(\epsilon \nu)$
$C_1, C_2,$ C_μ, C_D	coefficients involved in the turbulence model	R_{tur}	turbine radius
C_p	power coefficient based on the tower frontal area HD	t	time
C_{pt}	power coefficient based on the turbine area	T	axial thrust force on the turbine disc
C_T	disc-loading coefficient	u', v', w'	fluctuating values of radial, tangential, and axial velocity, respectively
D	tower internal diameter	U, V, W	mean values of radial, tangential, and axial velocity, respectively
D_{tur}	turbine diameter	v_∞	free stream wind velocity
g	gravitational acceleration	$w_{tur}(r)$	the axial velocity at radius r on the turbine exit
H	tower height	z	vertical location
H_d	height of computational domain	z_0	aerodynamic roughness of the site
i	radial number of a nodal point	Δr	mesh size in radial direction
j	vertical number of a nodal point	Δz	mesh size in axial direction
k	kinetic energy of turbulence per unit mass $k \equiv \frac{1}{2} (\overline{u'^2} + \overline{v'^2} + \overline{w'^2})$	ϵ	dissipation rate of turbulence energy
λ_D	dissipation length scale	μ	molecular viscosity
p	static pressure	μ_T	turbulent eddy viscosity
p_t	total pressure	μ_{eff}	effective viscosity $\mu_{eff} = \mu_T + \mu$
P	possible power output	ν	kinematic viscosity for air
r	radial location	ρ	density for air
R_i	swirl-Richardson number	$\sigma_k, \sigma_\epsilon$	turbulent Prandtl number for kinetic energy of turbulence and rate of dissipation, respectively.
R_o	outer radius of computational domain		